

Cathodoluminescence emission by cubic boron nitride crystals

Although cathodoluminescence effects in diamond crystals have been investigated in some detail [1–3], similar studies with cubic boron nitride have not been reported.

Cubic boron nitride has the same atomic arrangement as diamond and marked similarities can be observed in many of the physical properties of these materials. However, the structure of cubic boron nitride belongs to the space group $\bar{4}3m$ whereas diamond has $Fd\bar{3}m$ symmetry.

The colour of cubic boron nitride can be varied by suitably doping the crystals, and in a similar manner the crystal morphology can be rendered either predominantly octahedral or predominantly tetrahedral. However, in all cases, the preferred growth facets are of the form $\{111\}$.

In our own scanning electron microscope studies we have observed one form of cubic boron nitride which is interesting because of its unique cathodoluminescence response. These particular crystals are black in colour and have an octahedral habit (Fig. 1a) produced by almost equal development of the eight $\{111\}$ facets. In accordance with the known cathodoluminescence response in diamond, it might have been expected that all eight crystal faces would exhibit cathodolumi-

nescence in exactly the same way. However, as can be seen in Fig. 1b, this is not the case and, instead, only four faces cathodoluminesce strongly and the remaining $\{111\}$ facets respond either weakly or not at all to electron bombardment. Although the wavelength of the optical emission cannot be readily determined with the cathodoluminescence detector in the SEM, it was visually observed that the crystals glowed a deep blue-purple colour.

What is particularly interesting is the way in which the four strongly cathodoluminescent faces, and therefore the four darker facets also, are related to each other by four-fold inversion axes lying along the $\langle 100 \rangle$ axes of the crystals. Clearly, therefore, the cathodoluminescence response reflects the symmetry of the crystal structure even though the crystal habit does not.

The precise nature of the centres giving rise to the cathodoluminescence response of these crystals is not known, but it would seem that their distribution is dependent upon the atomic arrangement in cubic boron nitride.

Spinel twins, produced by a 180° lattice rotation about a $\langle 111 \rangle$ type direction, were a common feature with these particular crystals (Fig. 2a). The nature of their cathodoluminescence response (Fig. 2b) reflects the operation of the twin in that the bright and dark faces on one side of the twin boundary are related to those on the

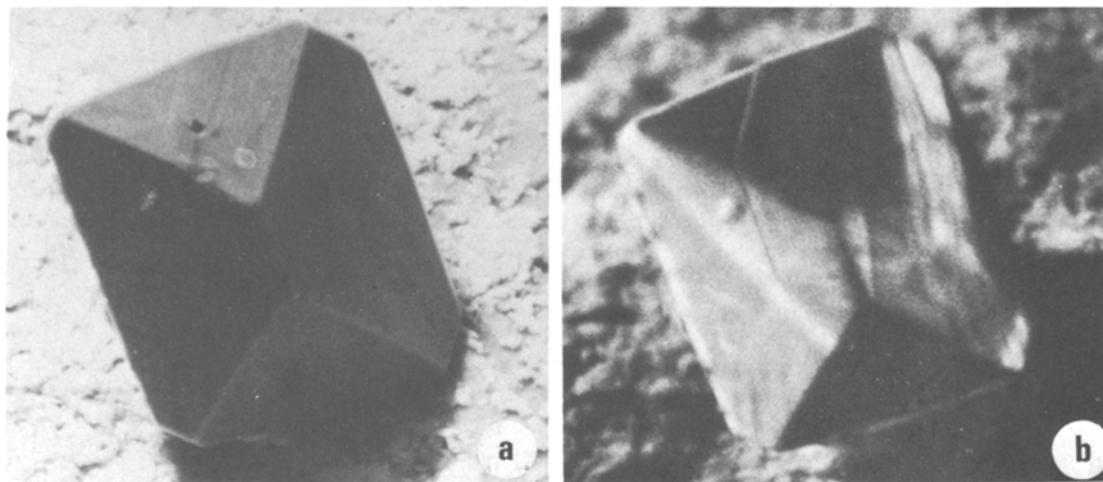


Figure 1 Octahedral cubic boron nitride crystal (a) and its cathodoluminescence image (b).

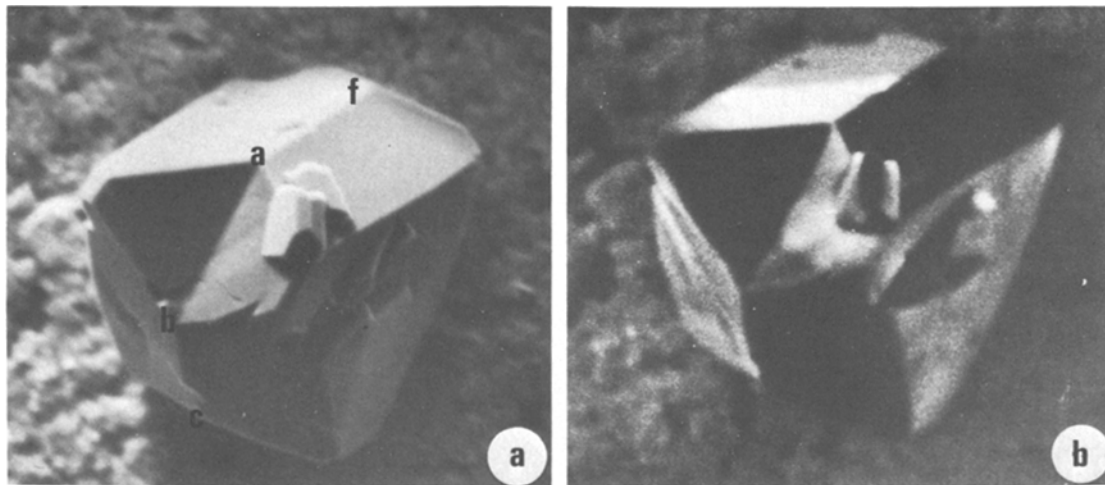


Figure 2 Cubic boron nitride spinel twin (a) and its cathodoluminescence image (b). The twin boundary is the plane $fabc$.

opposite side, again by a 180° rotation about the same $[1\ 1\ 1]$ axis.

Figs. 3a and b demonstrate schematically how the spinel twin cathodoluminescence emission develops from an octahedron with $\bar{4}$ cathodoluminescence symmetry. Clearly, therefore, as the lattice rotates during the formation of the twin, the defect distribution giving rise to these cathodoluminescence effects rotates with it. This is further

confirmation that the cathodoluminescence symmetry is defined by the atomic arrangement and, therefore, the lattice symmetry of the cubic boron nitride crystal structure.

These particular effects were observed only for the black-coloured material. In the other forms of cubic boron nitride which we have examined all of the eight $\{1\ 1\ 1\}$ facets were found to cathodoluminesce equally strongly.

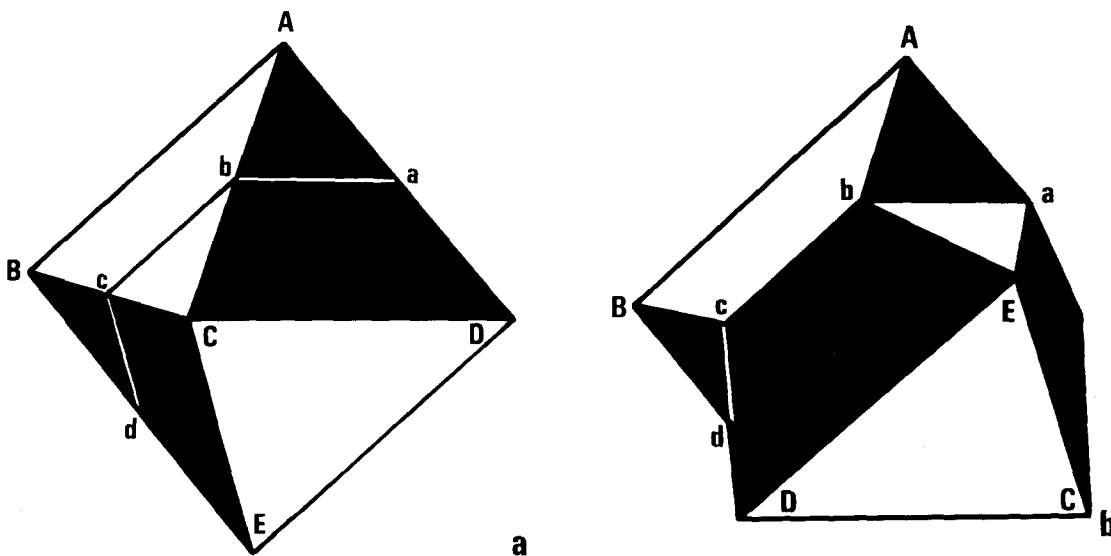


Figure 3 Schematic representation to show the formation of a spinel twin and the associated cathodoluminescence response of the various $\{1\ 1\ 1\}$ facets. The twin boundary is the plane $abcd$.

References

1. G. S. WOODS and A. R. LANG, *J. of Crystal Growth* 28 (1975) 215.
2. A. S. VISHNEVSKY, *ibid.* 29 (1975) 296.
3. P. L. HENLEY, I. KIFLAWI and A. R. LANG, *Phil. Trans. Roy. Soc. A* 284 (1977) 329.

Received 20 June 1979
and accepted 21 February 1980

N. J. PIPKIN
*De Beers Diamond Research Laboratory,
Johannesburg,
South Africa*

Variations of dynamic viscoelastic properties of dog compact bone during the fatigue process

The ability of bone to withstand repetitive loading is closely related to its fatigue fracture properties. For example, a fatigue fracture occurs in the metatarsal bone during marching, the so-called "march fracture". The relationship between stress amplitude and the number of cycles up to fatigue fracture (S-N curve) has been reported [1, 2] in addition to optical and electron microscopic observations of the fatigue fracture surface [3, 4]. The variation of mechanical properties and structure of compact bone during cyclic fatigue has not been reported. Such a study would be useful in clarifying the fatigue mechanism of compact bone. In this work, the variations of dynamic viscoelastic properties of dog compact bone during the fatigue process were investigated under various imposed dynamic strain amplitudes, and morphological observation of the fatigue fracture surface was carried out by scanning electron microscopy.

A tension-compression type fatigue tester was designed in order to carry out continuous measurements of dynamic complex modulus and mechanical loss tangent under the conditions of a constant ambient temperature and strain amplitude [5, 6]. Ten samples of adult dog compact bone were prepared from the metatarsal bone in the shape of a rectangular plate 5 mm wide, 2 mm thick, and 20 mm long in gauge length. The specimens were dried in a desiccator for 2 months. The tension-compression direction was coincident with the longitudinal direction of the compact bone. The fatigue testing frequency was 6.91 Hz and an ambient temperature was 295 K. The specimen temperature did not rise appreciably during fatigue testing. Morphological observation of fatigue fracture surface was carried out by using a scanning electron microscope, JEOL Model JSM-50A (Nippon Denshi Co., Ltd., Japan). The temperature dependence of dynamic loss modulus of the dry dog compact bone was measured with a dynamic viscoelastometer, Rheovibron Model DDV-III (Toyo Baldwin Co., Ltd., Japan).

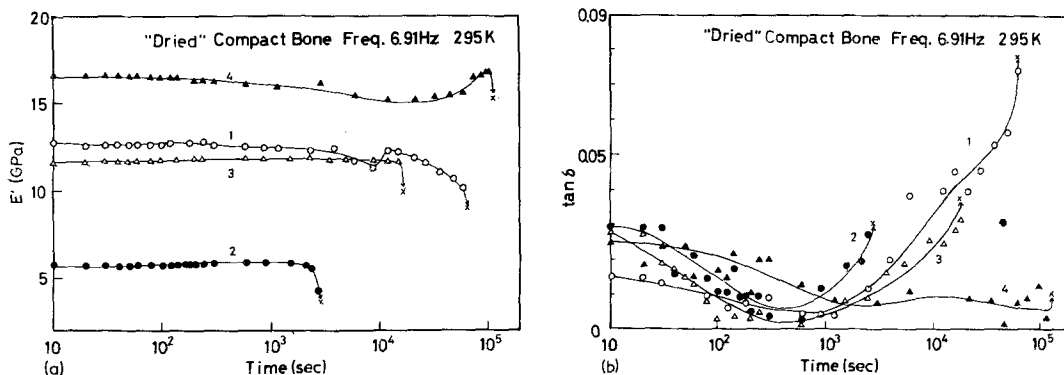


Figure 1 Variations of dynamic storage modulus, E' (a) and mechanical loss tangent, $\tan \delta$ (b) of "dried" compact bone with fatigue process at ambient temperature of 295 K. Strain amplitude: curve 1 (0.326%), curve 2 (0.315%), curve 3 (0.276%), curve 4 (0.175%).